Ganesh Thiagarajan[1]
Department of Civil and Mechanical Engineering,
University of Missouri-Kansas City,
350K Robert H. Flarsheim Hall,
5110 Rockhill Road,
Kansas City, MO 64110
e-mail: ganesht@umkc.edu

Mark T. Begonia
Department of Civil and Mechanical Engineering,
University of Missouri-Kansas City,
350K Robert H. Flarsheim Hall,
5110 Rockhill Road,
Kansas City, MO 64110

Mark Dallas
Department of Oral and Craniofacial Sciences,
School of Dentistry,
University of Missouri-Kansas City,
Room 3143, 650 E 25th Street,
Kansas City, MO 64108

Nuria Lara-Castillo
Department of Oral and Craniofacial Sciences,
School of Dentistry,
University of Missouri-Kansas City,
Room 3143, 650 E 25th Street,
Kansas City, MO 64108

JoAnna M. Scott
Department of Oral and Craniofacial Sciences,
School of Dentistry,
University of Missouri-Kansas City,
Room 3143, 650 E 25th Street,
Kansas City, MO 64108

Mark L. Johnson
Department of Oral and Craniofacial Sciences,
School of Dentistry,
University of Missouri-Kansas City,
Room 3143, 650 E 25th Street,
Kansas City, MO 64108

Determination of Elastic Modulus in Mouse Bones Using a Nondestructive Micro-Indentation Technique Using Reference Point Indentation

The determination of the elastic modulus of bone is important in studying the response of bone to loading and is determined using a destructive three-point bending method. Reference point indentation (RPI), with one cycle of indentation, offers a nondestructive alternative to determine the elastic modulus. While the elastic modulus could be determined using a nondestructive procedure for ex vivo experiments, for in vivo testing, the three-point bending technique may not be practical and hence RPI is viewed as a potential alternative and explored in this study. Using the RPI measurements, total indentation distance (TID), creep indentation distance, indentation force, and the unloading slope, we have developed a numerical analysis procedure using the Oliver–Pharr (O/P) method to estimate the indentation elastic modulus. Two methods were used to determine the area function: (1) Oliver–Pharr (O/P—based on a numerical procedure) and (2) geometric (based on the calculation of the projected area of indentation). The indentation moduli of polymethyl methacrylate (PMMA) calculated by the O/P (3.49–3.68 GPa) and geometric (3.33–3.49 GPa) methods were similar to values in literature (3.5–4 GPa). In a study using femurs from C57Bl/6 mice of different ages and genders, the three-point bending modulus was lower than the indentation modulus. In femurs from 4 to 5 months old TOPGAL mice, we found that the indentation modulus from the geometric (5.61 ± 1.25 GPa) and O/P (5.53 ± 1.27 GPa) methods was higher than the three-point bending modulus (5.28 ± 0.34 GPa). In females, the indentation modulus from the geometric (7.45 ± 0.86 GPa) and O/P (7.46 ± 0.92 GPa) methods was also higher than the three-point bending modulus (7.33 ± 1.13 GPa). We can conclude from this study that the RPI determined values are relatively close to three-point bending values. [DOI: 10.1115/1.4039982]

1 Introduction

Aging produces a general decline in the mechanical integrity of bones, but diseases such as osteoporosis and osteogenesis imperfecta accelerate bone deterioration thereby causing them to become more prone to fracture. Mechanical testing of whole bones (e.g., axial compression and bending) in mouse models have relied on ex vivo experiments to determine mechanical properties such as elastic modulus and susceptibility to fracture. Mouse models are advantageous for studying bone properties because their genetic backgrounds are tightly controlled and their relatively smaller size can facilitate testing procedures. In addition, longitudinal studies can be conducted to study aging effects on bone.

One of the traditional methods for analyzing the mechanical properties of bone is the three-point bending test in which a bone is placed over two fixed supports separated by a known distance and then loaded through a third point of contact usually at the midshaft [1–5]. Although nondestructive tests can be done on bones to determine the elastic modulus, destructive testing is usually performed in order to determine other structural and properties. The three-point bending test is therefore not appropriate for in vivo testing since it cannot be used longitudinally within the same mouse as it ages. A study by Hansma et al. [6] reported the use of a device that was designed to analyze the mechanical properties of bone in vivo. This device utilized a methodology known as reference point indentation (RPI) wherein a reference probe was positioned on the bone surface to identify the reference point while an inner test probe was driven into the bone and collected various measurements based on micro-indentation testing principles.

Various studies have been performed in the past several years to explore the application of RPI on cadaver tissue. Buetel and Kennedy [7] studied the measurements given by the RPI instrument and the resulting RPI variables such as the loading slope, first cycle indentation distance (ID1), total indentation distance

[1]Corresponding author.
Manuscript received February 20, 2017; final manuscript received April 2, 2018; published online May 10, 2018. Assoc. Editor: David Corr.

(TID), mean energy dissipation, first cycle unloading slope (US1), and mean unloading slope (US). They observed micro damage that was consistent at the indentation sites, which increased with increasing number of cycles. Karim et al. [8] studied the associations between RPI variables, cortical bone density, and morphology in human tibia and femurs. Katsamenis et al. [9] investigated the osteonal-, micro-, and tissue-level mechanical behavior of cortical bone tissue samples from young and elderly donors using nano-indentation, RPI, and fracture toughness experiments. They reported that apparent bone material toughness obtained from three-point bending and axial compression tests was inversely correlated with the indentation distance increase (IDI) obtained from RPI. Granke et al. [10] showed a significant correlation between IDI and ultimate stress and toughness in femoral bones at the midshaft region. Granke et al. [11] used a multimodality approach to assess the fracture toughness of human cadaveric bones by using techniques appropriate to different length scales of bone, as a means to complement the dual X-ray density absorptiometry measurements used to get the areal bone mass density, which is currently used to assess fracture risk in a clinical setting. They used clinical magnetic resonance imaging to quantify hydration and porosity as a metric to determine fracture toughness and cyclic RPI to measure bone's material properties and have suggested that different modalities are sensitive to different features of the bone. Correlation values between properties of fracture toughness and various RPI parameters were determined. Diez-Perez et al. [12] studied the effect of RPI variables in vivo on human female bones by showing differences between osteoporotic and normal bones as well as demonstrating its feasibility in clinical settings. Using specimen from fresh-frozen cadaveric femoral bones, Krege et al. [13] explored the relationship between cyclic RPI parameters such as IDI and ultimate load and traditional biomechanical properties from four-point bending tests under various experimental conditions such as bone demineralization and soaking in raloxifene, drying, and ashing. The study showed that there was no clear IDI value or a trend in IDI value that could relate the clinically relevant bone changes to the fracture properties of the whole bone.

Several animal models have also been studied. Gallant et al. [14] correlated the results obtained by RPI with those of traditional mechanical testing, namely three-point bending and axial compression on rat and canine bones. Allen et al. [15] studied in vivo measurement of Sprague–Dawley rats to assess intra- and inter-animal variability. Carriero et al. [16] investigated the relationship between fracture toughness and RPI parameters from mice of six different strains and suggested that RPI variables are not indicative of stress intensity fracture toughness in mouse bone.

Allen et al. [17] in their review article discussed that while RPI represented a new and innovative technology with a potential to clinically assess mechanical properties of bone, there were several questions about the relationship between RPI measurements and traditional mechanical properties. Idkaidek et al. [18] have used finite element methods to study the relationship between various RPI parameters and the elastic modulus and found the unloading slope (US) to be a good direct indicator while ID1 and TID were inversely related to the elastic modulus. Jenkins et al. [19] studied the dependence of IDI on several testing parameters such as maximum load, sample orientation, mode of use, sample preparation, and measurement spacing, in order to suggest effective protocols and reduce the effect of confounding factors. In a subsequent study, Jenkins et al. [20] suggested that various RPI measures represented different properties reflective of bone quality but were not strongly correlated to a single mechanical property.

We have attempted to address the question related to the utility of RPI to one of the mechanical properties in this research and shed some light on how the RPI measurements can be related to traditional mechanical properties such as the elastic modulus in a nondestructive manner. This methodology is novel as it has the potential to be applied to in vivo longitudinal studies in mouse bones.

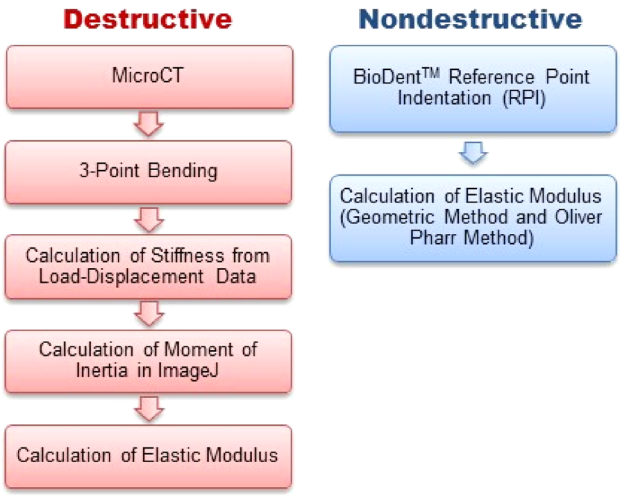

Fig. 1 Comparison of destructive (to determine structural properties of the bone) versus nondestructive methods of determining the elastic modulus in bone

In the current study, we have used the RPI technique in conjunction with the principles of indentation from the classical Oliver–Pharr [21] technique to measure the elastic modulus of the mouse bone. We have modified the recommended RPI protocol to apply multiple cycles of load and instead use only a single cycle of load and use several parameters of the load-indentation curve to calculate the elastic modulus. This paper presents the mechanical properties of various mouse bones across different strains/genotypes that were obtained through our RPI technique and then compared with the elastic modulus obtained from conventional three-point bending tests. The overall research goal is to develop a reliable, nondestructive in vivo method of determining the elastic modulus in mouse bones. Figure 1 outlines the steps involved in both the destructive (that we currently use to determine the elastic modulus and other structural properties on ex vivo specimen) and the proposed nondestructive testing methods—which shows several complexities involved with the three-point bending modulus determination. Apart from the destruction of the bone during three-point bending, the conventional destructive procedure requires additional analysis steps (e.g., determination of the moment of inertia (MOI) using microCT scans) in order to calculate the elastic modulus. In contrast, the proposed nondestructive procedure is a simple two-step process that can be carried out in vivo on the RPI instrument if needed and involves simpler calculations. The purpose of this study was not to determine whether three-point bending or RPI was better for detecting changes in tissue modulus, but to obtain the bone properties using a nondestructive test and to determine whether these calculations were similar to those obtained using standard methods (three point bending). The primary advantage of the technique is that one can follow the same animal/bone in a longitudinal study to track the property over time while the disadvantage is that RPI may not be suitable for examining the fracture resistance.

2 Materials and Methods

The BioDent™ *Hfc* (ActiveLife Scientific, Inc., Santa Barbara, CA) [6,22] RPI platform was used to perform various studies on different strains of mouse bones as well as polymethyl methacrylate (PMMA) samples. The samples chosen have an elastic modulus similar to that of bone. Figure 2 shows the RPI system with the bone in a secured water bath and the custom fixtures used in this study. The BP-2 type of test and reference probe was used for this study. In order to minimize damage to the samples, the

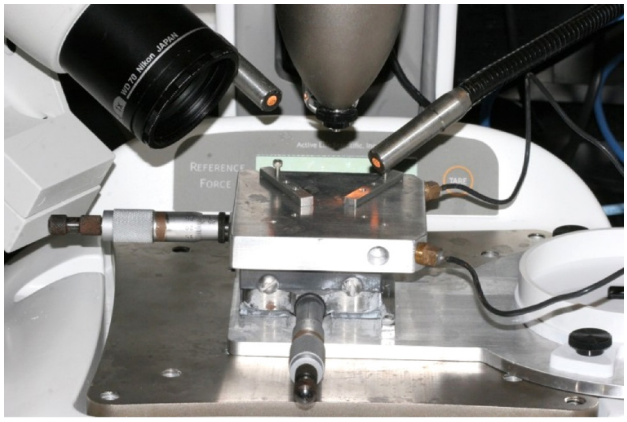

(*a*)

(*b*)

Fig. 2 Reference Point Indentation instrument used along with the custom positioning fixture built for the study with the microscope (top) and the bone during the indentation process (bottom)

reference probe has a blunted end. In a review paper by Allen et al. [17], the authors suggest BP-2 probes for ex vivo work on large bones, and BP-3 probes for small animal work—based on manufacturer's recommendations. However, based on a local visit by the company representative, BP-2 probes were recommended by the company. In addition, we tested the BP-3 probes but the BP-2 probes performed better at 2 N and were more stable on the bone surface during testing. Using 2 N (1 cycle) load did not cause any issues with specimen damage. The custom fixture included the two Vernier caliper platforms for securing the bone/sample at the desired location. This setup also allowed for accurate positioning of each indentation site on the bone surface so that the RPI measurements and elastic modulus could be determined along the length of the bone.

2.1 Polymethyl Methacrylate and Mouse Bone Groups. In order to establish the RPI methodology and test it prior to its application to mouse bones, we conducted preliminary studies on PMMA samples provided by the manufacturers of the BioDent Reference Point Indentation testing platform. After confirming the repeatability of the methodology and the accuracy of the elastic modulus calculation, we conducted three different studies on different strains of mouse bones. Bone samples were collected from several previous and ongoing studies conducted by our group. Bones were wrapped in saline soaked gauze and frozen ($-20\,^{\circ}C$) immediately after they were harvested. Prior to actual testing, bones were thawed and then removed of their soft tissue.

The first study (group 1) consisted of ulnas that were harvested from 6 months old female TOPGAL mice. These mice are maintained in our colony on a mixed C57BL6 $\times$ CD1 background, serve as a reporter for the β-catenin signaling pathway, and are used for various related studies [23]. The sample size for group 1 was relatively small ($n = 3$) because this group was part of an initial study to test the feasibility of applying this technique on mouse bones. In addition to obtaining RPI measurements, we performed scanning electron microscopy (SEM) to assess changes on the ulna surface caused by each indentation. The variation of the elastic modulus along the length of the ulna was studied for this group. We have used the ulna as it is being studied extensively in our labs. We have used it to conduct several in vivo and ex vivo loading experiments for the detection of biological markers and the determination of mechanical properties using the three-point bending tests [23,24]. Several of our past and proposed publications have used the ulna for correlating strains determined experimentally and using finite element methods [25,26].

In the second study (group 2), age effects on the elastic modulus of bone were analyzed in femurs that were collected from C57BL/6 mice (National Institutes of Health, Bethesda, MD) at 6 months ($n = 6$ female/male), 12 months ($n = 6$ female/male), and 22 months ($n = 7$ female/male) old.

The final study (group 3) was conducted on femurs ($n = 3$, female/male) collected from β-catenin heterozygous conditional knockout (HETcKO) mice. Femurs were obtained from 4–5-month-old heterozygous conditional knockouts (Dmp1-Cre (+) $\times$ β-catenin fl/+ in a C57BL/6 background) and their littermate controls (Dmp1-Cre (−) $\times$ β-catenin fl/+ in a C57BL/6 background). The β-catenin fl/fl (exon 2–6) mice were purchased from Jackson Laboratories (B6.129—Catnbtm2Kem/J; Jackson Laboratories, Bar Harbor, ME). These animals were crossed with 10 Kb Dmp-1 Cre mice to obtain mice with heterozygous deletion of β-catenin in osteocytes. Out of this cross, mice bearing the Cre gene were identified as HETcKO and littermates that were negative for Cre gene were identified as control.

All animal experiments were approved by the UMKC Animal Care and Use Committee.

2.2 Reference Point Indentation Method. Reference point indentation tests are routinely performed on PMMA, before and after RPI tests are performed on bone, in order to ensure the quality and stability of the test probe. During RPI testing of bones, each sample was secured onto a custom stage and submerged in phosphate buffered saline while a dissection microscope (Nikon SMZ800) was used to position the reference probe over each indentation site. Multiple indentation sites were selected along the shaft of each bone to investigate regional differences in mechanical properties. Each indentation site was approximately 1 mm apart. The instrument can apply an indentation force ranging from 2 N to 10 N. However, each indentation in this study was generated by applying a reference load applied by the reference probe, based on the specifications of the instrument and the indentation force of 2 N was applied for one cycle. The maximum load of 2 N was selected because it was determined to be the appropriate force to apply without causing damage to the bone surface as noted by several researchers [14,27]. Only one cycle was applied since data from a single indentation are sufficient to calculate the elastic modulus [17].

2.3 Reference Point Indentation Data Analysis. The elastic modulus was calculated from RPI measurements using the Oliver–Pharr technique but two different methods were used to determine the area function that is required. The two aforementioned methods are referred to as the (1) Oliver–Pharr method and (2) geometric method—in this paper. The Oliver–Pharr (O/P) technique [21] was developed by Warren C. Oliver and George M. Pharr to determine the elastic modulus and hardness of a

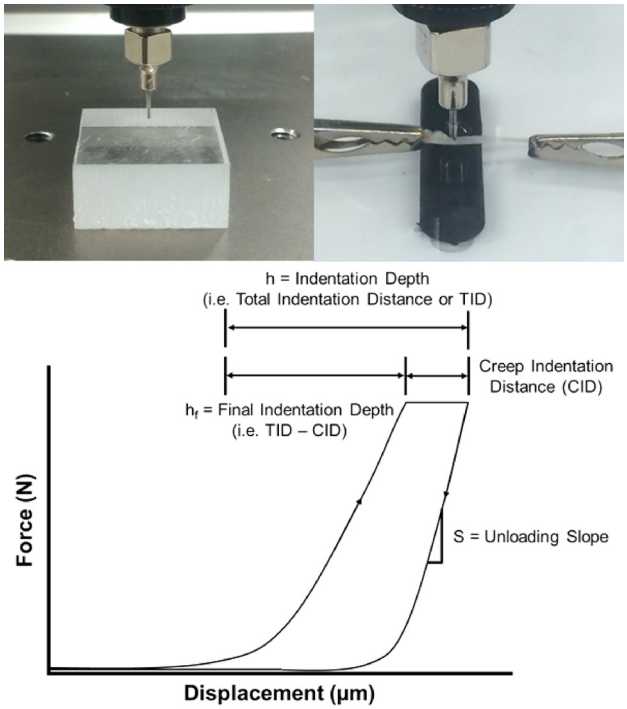

Fig. 3 Reference point indentation indenter prior to indentation in PMMA block (Top left), indentation on mouse bones, which are held in place by grips (Top right) and a typical one cycle indentation curve output by the RPI instrument from which material parameters are determined

material using load–displacement data from a single cycle of indentation. The accuracy of the elastic modulus is dependent on the maximum load, maximum displacement, and elastic unloading stiffness (i.e., contact stiffness) [21,28]. Figures 3(*a*) and 3(*b*) show the indentation on a sample of PMMA and mouse ulna, respectively. Figure 3(*c*) shows the first cycle load-indentation curve and the parameters measured by the RPI instrument, namely the initial indentation distance (ID1), TID, and creep indentation distance that were used for the determination of the indentation elastic modulus. The data from the RPI instrument were exported as a text file and a custom script was developed to automatically compute the indentation elastic modulus based on the Oliver–Pharr method [28]. The data from the unloading part of the curve were first fitted to a power law function as shown in the below equation:

$$P = \alpha(h - h_f)^m \tag{1}$$

where P is the indentation force, h is the TID, h_f is the final indentation depth and is equal to TID-creep indentation distance, and α and m are the power law fitting constants. The contact depth h_c is required for the contact area function A and is given by the below equation:

$$h_c = h_f - \epsilon\frac{P_{\max}}{S} \tag{2}$$

where $P_{\max}$ is the peak indentation load, ε is a geometric constant for the conical indenter and is equal to 0.72 [21], and S is the unloading slope at the peak indentation force as shown in Fig. 3. The area functions that have been tested in this work are based on two different methods, namely the Oliver–Pharr method (designated as the O/P method) given by Eq. (3) and the projected area of the geometry of the cone as shown in Eq. (4) is referred to as the geometric method in this paper. The slope in Eq. (4) represents the slope of the incline of the conical indenter surface. The radius r_o in Eq. (4) for the indenter used is 2.5 μm

$$A = C_o h_c^2 \tag{3}$$

$$A = \pi(r_o + \text{slope} * h_c)^2 \tag{4}$$

For the conical indenter, the constant C_o was calibrated based on the elastic modulus values of PMMA and was determined to have a value of 3. Only one indentation was performed at each site to reduce wear and tear on the indenter tip. Although the manufacturer's recommended use for each RPI tip (maximum of 80 indents per tip) was never exceeded, it should be mentioned that C_o parameter may not be a true constant. Future work will examine this issue in greater detail. Based on the variables calculated in Eqs. (1)–(4), the reduced elastic modulus can be expressed as described in the Oliver–Pharr method [21] and shown in the below equation:

$$E_r = \frac{\sqrt{\pi}S}{2\sqrt{A}} \tag{5}$$

From the reduced elastic modulus, the indentation elastic modulus E for the bone is computed as shown in the below equation:

$$\frac{1}{E_r} = \frac{1-\nu^2}{E} + \frac{1-\nu_i^2}{E_i} \tag{6}$$

where the subscript i represents the values of Poisson's ratio and the elastic modulus of the indenter. In this work, the indenter is made of steel. Hence, the value of E_i is set to 200 GPa while the Poisson's ratio is set to 0.3. Since it is difficult to determine the Poisson's ratio of bone, the value is set to 0.17 based on its usage in literature [29,30].

2.4 Biomechanical Analysis. In addition to reference point indentation, we determined the elastic modulus of bones using a biomechanical analysis procedure that employed microCT, three-point bending, and the BoneJ plug-in for ImageJ (National Institutes of Health, Bethesda, MD) [31,32]. All bones were scanned via microCT (SkyScan 1174, Bruker microCT, Kontich, Belgium) at an in-plane resolution of 9.6 μm and axial slice spacing of 9.6 μm, which produced a voxel volume of approximately 884 μm^3. SkyScan programs such as NRecon and CT-analyser were then used to perform image reconstruction and contouring, respectively. A Bose ElectroForce 3220 system (TA Instruments, ElectroForce Systems Group, Eden Prairie, MN) was used to conduct three-point bending, as shown in Figure 4(*a*), using a preload of 0.5 N and a displacement rate of 0.1 mm/s. After obtaining the stiffness from the resulting load–displacement data, we calculated the elastic modulus (E) using the below equation:

$$E = \frac{Kl^3}{48I} \tag{7}$$

where K represents the stiffness as shown in Fig. 4(*b*), l represents the span (i.e., distance between the supports), and I represents the moment of inertia about the bending axis. BoneJ was then used to realign the microCT image stack with respect to the bone's longitudinal axis and then calculate the area moments of inertia for 11 bone slices that were spaced apart equally across the span as shown in Fig. 4(*c*). An average value for the moment of inertia was calculated after analyzing one slice that was centrally located at the midshaft, five slices that were distal to the midshaft, and five slices that were proximal to the midshaft.

2.5 Statistical Analysis. Pearson correlation coefficients were calculated to determine the correlation between elastic

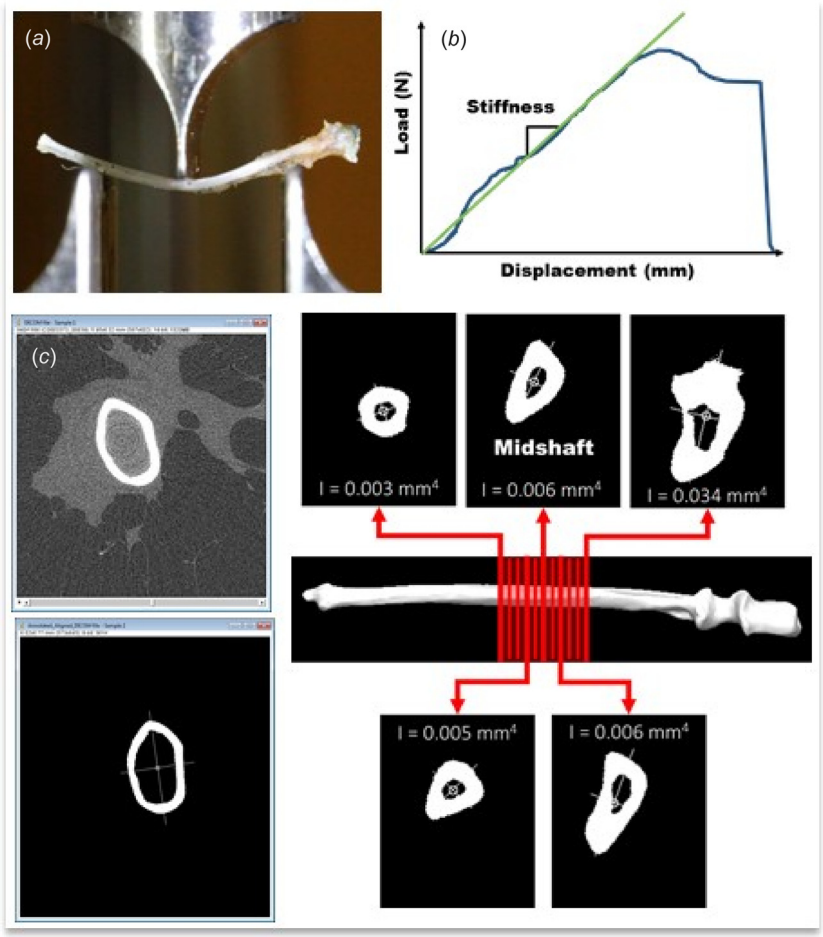

Fig. 4 (*a*) First, microCT scanning and three-point bending are employed. (*b*) Second, the stiffness is obtained from the load–displacement data. (*c*) Third, BoneJ is used to realign microCT slices and obtain an average moment of inertia that is used for calculating the elastic modulus.

modulus values obtained from three-point bending versus the proposed RPI methods by gender (male and female), age (6 months, 12 months, and 22 months), and location (all indentation sites, only midshaft sites, only proximal sites, and only distal sites).

One way analysis of variance (ANOVA) was used to determine if there were differences in elastic modulus values by location (only midshaft sites, only proximal sites, and only distal sites) for each of the three methods (three-point bending, geometric method, and O/P method) overall and by gender. The significance level was set to 0.05. All analyses were performed in Stata 14.1 (StataCorp LP., College Station, TX).

3 Results

This section provides details from various studies in which the elastic modulus was determined through three-point bending and/or the RPI technique. At the outset, two preliminary studies conducted on PMMA and TOPGAL mouse bones to verify the RPI methodology are presented. Subsequently, more detailed studies involving two groups of mice are presented in an attempt to validate and correlate the methodology with the elastic modulus obtained from conventional three-point bending tests.

Table 1 Summary of elastic modulus values obtained from two RPI analysis techniques and literature for PMMA

Literature	Geometric method	Oliver–Pharr (O/P) method
3.5–4.0 GPa	3.33–3.49 GPa	3.49–3.68 GPa

3.1 Analysis of Polymethyl Methacrylate. Table 1 shows that the elastic moduli calculated using the RPI technique and both methods of calculating the area function compared well with values reported previously for PMMA. The area function coefficient C_o has been calibrated to match the elastic modulus values of PMMA. Furthermore, the ranges in elastic moduli suggest that the O/P method yields a slightly higher elastic modulus (4.8–5.4%) compared to the geometric method.

3.2 Group 1—Ulna From TOPGAL Mice. Table 2 summarizes the RPI moduli obtained from the TOPGAL ulna based on the location of the indentation site. The RPI technique was able to capture regional differences on the ulna surface, which was evidenced by higher elastic moduli for the midshaft compared to either the distal or proximal locations. In addition, the O/P method

Table 2 Summary of elastic modulus values obtained from two BioDent analysis techniques for TOPGAL mice

	Geometric method	Oliver–Pharr (O/P) method
Proximal	4.24 GPa	4.66 GPa
Midshaft	5.08 GPa	5.71 GPa
Distal	4.51 GPa	4.97 GPa

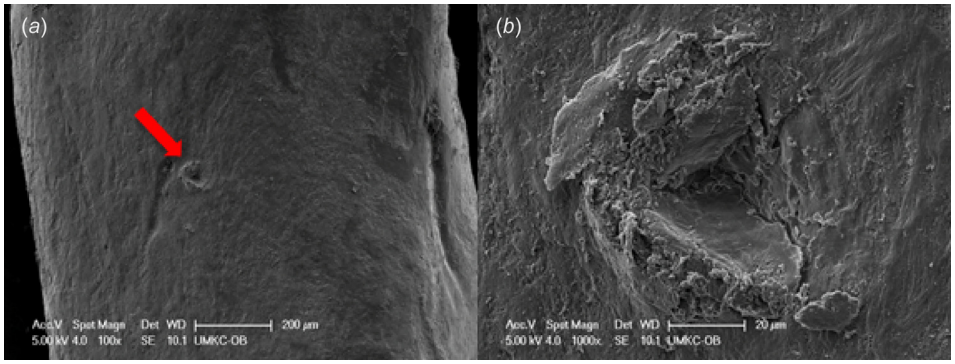

Fig. 5 Scanning electron microscopy micrographs showing the indentation location and microcracks at (*a*) 100× and (*b*) 1000× on the TOPGAL ulna. A 2 N load was applied for 1 cycle.

Table 3 Comparison of elastic modulus values obtained from three-point bending versus the proposed RPI methods in C57BL/6 male femurs. Elastic modulus values calculated with the RPI technique collected from (*a*) all indentation sites (*b*), only midshaft sites, (*c*) only proximal sites, and (*d*) only distal sites.

		Elastic modulus		
Gender and age	Indentation sites included	Geometric method	O/P method	Three-point bending
Male 6 months ($n = 6$)	All indentation sites	5.87 ± 1.13	6.69 ± 1.35	4.97 ± 0.80
Male 12 months ($n = 6$)		5.55 ± 1.86	6.35 ± 2.29	4.85 ± 1.32
Male 22 months ($n = 7$)		5.31 ± 1.22	6.11 ± 1.46	3.34 ± 0.66
Male 6 months ($n = 6$)	Midshaft sites only	6.03 ± 1.10	6.84 ± 1.29	4.97 ± 0.80
Male 12 months ($n = 6$)		5.96 ± 2.18	6.81 ± 2.69	4.85 ± 1.32
Male 22 months ($n = 7$)		5.87 ± 1.01	6.78 ± 1.20	3.34 ± 0.66
Male 6 months ($n = 6$)	Proximal sites only	6.20 ± 1.52	7.11 ± 1.83	4.97 ± 0.80
Male 12 months ($n = 6$)		5.44 ± 1.93	6.22 ± 2.38	4.85 ± 1.32
Male 22 months ($n = 7$)		5.41 ± 1.32	6.18 ± 1.59	3.34 ± 0.66
Male 6 months ($n = 6$)	Distal sites only	5.39 ± 0.60	6.12 ± 0.76	4.97 ± 0.80
Male 12 months ($n = 6$)		5.24 ± 1.73	6.02 ± 2.12	4.85 ± 1.32
Male 22 months ($n = 7$)		4.65 ± 1.16	5.36 ± 1.40	3.34 ± 0.66

tended to report slightly higher elastic moduli at the proximal (9.9%), midshaft (12.4%), and distal (10.2%) indentation sites compared to the geometric method. As stated earlier, no statistics are reported for this group of mice because this series of experiments was used initially to test the feasibility of the methodology.

Figure 5 shows the SEM micrographs from the surface of the TOPGAL mouse ulna at (*a*) 100× and (*b*) at 1000× after applying a 2 N load for 1 cycle. The indentation site (indicated by an arrow in Figure 5(*a*)) was positioned centrally along the longitudinal axis of the ulna. The corresponding microdamage was approximately 25–30 μm wide.

3.3 Group 2—Femurs From C57BL/6 Mice. In the second group, we determined the elastic moduli using the RPI analysis technique and subsequently performed three-point bending on C57BL/6 mouse femurs. The femurs were collected from three age groups—6 months ($n = 6$ female/male), 12 months ($n = 6$ female/male), and 22 months ($n = 7$ female/male). These mice were part of a broader study involving the effects of aging on bone and muscle. For the current study, we performed RPI tests on each femur at three locations on the bone surface—namely the proximal, midshaft, and distal sites. The proximal and distal sites were approximately 2–3 mm from the midshaft. Tables 3 and 4 show the RPI indentation modulus based on the measurements collected from all indentation sites as well as the midshaft, proximal, and distal indentation sites. The male femur data in Table 3 showed that when all indentation sites were included, the three-point bending modulus was generally lower compared to the moduli obtained through the RPI analysis technique. For the 6-, 12-, and 22-month groups, the three-point bending modulus was lower by 15%, 12.6%, and 37%, respectively, if the geometric method was applied and lower by 25.7%, 23.6%, and 45%, respectively, if the O/P method was applied. The midshaft sites generally produced a higher modulus compared to the distal and proximal sites. When comparing the 12- and 22-month groups (Table 3), three-point bending appeared to be more sensitive to detecting an age-related decline in the elastic modulus compared to the RPI analysis technique. As expected, the three-point bending modulus also gradually decreased with aging while the moduli from the RPI analysis technique exhibited similar declines. When examining only the midshaft indentation sites of the 22-month group, we found that the three-point bending modulus was 43.1% lower than the RPI modulus from the geometric method and 50.7% lower than the RPI modulus from the O/P method.

The female femur data in Table 4 showed a consistent decrease in the three-point bending modulus with aging, which was similar to the trend observed previously in the male femurs [33]. When focusing only on the midshaft sites and the 22-month groups, we found that the three-point bending was 17.5% lower than the RPI modulus calculated through the geometric method and 29.4% lower than the RPI modulus calculated through the O/P method.

Figure 6 shows a comparison of the elastic modulus values obtained either through three-point bending tests or the RPI technique (O/P method) according to gender and age. On comparing the modulus values between the genders, no apparent gender differences found in three-point bending data at 12 or 22 months of age but at 6 months, three-point bending shows that females have

Table 4 Comparison of elastic modulus values obtained from three-point bending versus the proposed RPI methods in C57BL/6 female femurs. Elastic modulus values calculated with the RPI technique are based on indentation data collected from (A) all indentation sites, (B) only midshaft sites, (C) only proximal sites, and (D) only distal sites.

		Elastic modulus		
Gender and age	Indentation sites included	Geometric method	O/P method	Three-point bending
Female 6 months ($n=6$)	All indentation sites	5.24 ± 1.09	6.03 ± 1.34	7.63 ± 0.78
Female 12 months ($n=6$)		5.10 ± 1.73	5.89 ± 2.08	5.09 ± 0.61
Female 22 months ($n=7$)		5.06 ± 0.86	5.90 ± 1.05	4.33 ± 1.34
Female 6 months ($n=6$)	Midshaft sites only	5.20 ± 1.09	6.01 ± 1.36	7.63 ± 0.78
Female 12 months ($n=6$)		4.98 ± 2.17	5.74 ± 2.65	5.09 ± 0.61
Female 22 months ($n=7$)		5.25 ± 0.67	6.14 ± 0.80	4.33 ± 1.34
Female 6 months ($n=6$)	Proximal sites only	4.84 ± 1.14	5.56 ± 1.40	7.63 ± 0.78
Female 12 months ($n=6$)		5.16 ± 2.16	5.94 ± 2.60	5.09 ± 0.61
Female 22 months ($n=7$)		5.09 ± 0.92	5.95 ± 1.12	4.33 ± 1.34
Female 6 months ($n=6$)	Distal sites only	5.67 ± 1.07	6.51 ± 1.32	7.63 ± 0.78
Female 12 months ($n=6$)		5.16 ± 0.84	5.99 ± 0.98	5.09 ± 0.61
Female 22 months ($n=7$)		4.84 ± 1.08	5.62 ± 1.35	4.33 ± 1.34

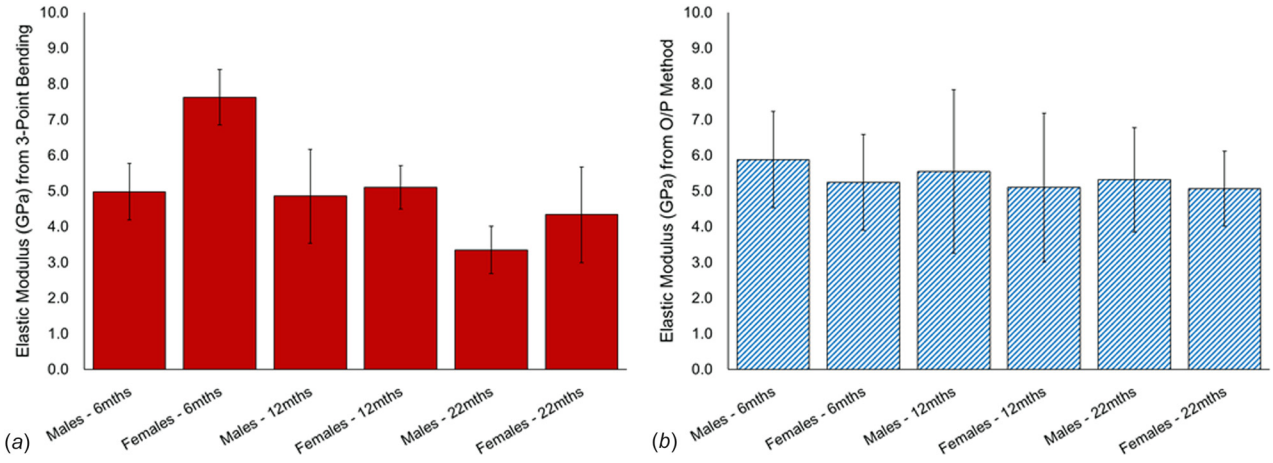

Fig. 6 Comparison of elastic moduli obtained from (*a*) three-point bending and (*b*) O/P method

a 53% higher elastic modulus than males. However, the RPI technique (i.e., both the O/P method and Geometric method) do not seem to detect gender-based differences in the elastic modulus for any age group.

3.3.1 Elastic Modulus by Location. Analysis of variance was used to determine whether there were differences in mean elastic modulus values by location. There was not a significant difference in mean elastic modulus values by location for any of the methods (geometric method ($p=0.37$), or O/P method ($p=0.36$)). There was still not a significant difference in mean elastic modulus values by location after stratifying by gender (For males: geometric method ($p=0.09$), or O/P method ($p=0.13$); for females: geometric method ($p=0.99$), or O/P method ($p=0.98$)) (data not shown).

3.3.2 Correlation Analysis. The results of the correlation analysis between the three methods of analysis are shown in Table 5. There is very strong correlation between the 2 RPI methods (Pearson correlation >0.99 in females and >0.95 in males) for all ages and locations. There is mild to moderate correlation between the two RPI methods and the three-point bending method. The magnitude of the Pearson correlation ranges from 0.005 (O/P versus three-point bending in 12-month-old females in the proximal location) to 0.699 (Geometric versus three-point bending in 22-month-old males in the proximal location) (Table 5).

Two other variables that are measured during RPI testing and then used to compute the RPI modulus are the initial unloading slope and the maximum indentation height. We have studied the variation of these parameters for the group three animals and made a few observations on the results shown in Table 6. First, the unloading slope in general reduces in value with aging irrespective of gender. Female bone specimens tended to have lower unloading slope values compared to males. The maximum indentation distances also were lower for female specimens compared to males, but this reduction was less than 5%. Another observation was that the maximum indentation height decreased with age regardless of gender, and with this decline was also less than 5%.

3.4 Group 3—Femurs From Heterozygous Conditional Knockout Mice. For this final group, we performed RPI tests on HETcKO mouse femurs ($n=6$ female/male) with the indentations located at the mid-diaphysis region. The results from this series of experiments are shown in Table 7. For the three-point bending tests (referred to as the three-point bending in Table 7), we used the same bones after performing the RPI indentation tests.

Two observations can be made from the data in Table 7. The first is that the modulus comparisons between the three-point bending method and both RPI analysis methods are almost all within a 5% difference. The only exception was found in the female HETcKO mice, which showed an elastic modulus that was 17% higher when applying three-point bending versus the RPI technique. Second, both techniques were able to capture differences in the elastic modulus values observed between the control and the conditional knock out mice for both the genders. Figure 7

Table 5 Pearson correlation between elastic modulus values obtained from three-point bending versus the proposed RPI methods C57BL/6 femurs stratified by gender (male and female), age (6 months, 12 months, and 22 months) and location (all indentation sites, only midshaft sites, only proximal sites, and only distal sites)

Elastic modulus methods	Gender	Age (months)	All indentation sites	Distal sites only	Midshaft sites only	Proximal sites only
Geometric versus O/P	Male	6	0.995	0.987	0.994	0.996
		12	0.999	0.996	1.000	0.999
		22	0.977	0.996	0.997	0.948
Geometric versus three-point bending		6	0.080	0.409	0.013	0.020
		12	−0.375	−0.224	−0.524	−0.363
		22	0.120	0.205	−0.652	0.699
O/P versus three-point bending		6	0.120	0.457	0.040	0.066
		12	−0.359	−0.157	−0.526	−0.354
		22	0.052	0.156	−0.691	0.534
Geometric versus OP	Female	6	0.998	—	0.998	0.999
		12	0.999	—	0.999	0.999
		22	0.996	—	0.991	0.997
Geometric versus three-point bending		6	0.286	—	0.278	0.290
		12	0.116	—	0.322	−0.018
		22	−0.150	—	−0.282	−0.112
O/P versus three-point bending		6	0.306	—	0.308	0.306
		12	0.123	—	0.316	−0.005
		22	−0.093	—	−0.242	−0.049

Table 6 Comparison of unloading slope (S) and maximum indentation height (h_f) based on gender, age, and indentation sites included

RPI parameter	Gender	Age (months)	All indentation sites	Midshaft sites only	Proximal sites only	Distal sites only
Unloading slope, S (N/μm)	Male	6	0.28 ± 0.05	0.29 ± 0.06	0.28 ± 0.06	0.26 ± 0.04
		12	0.26 ± 0.04	0.28 ± 0.05	0.26 ± 0.03	0.24 ± 0.05
		22	0.23 ± 0.05	0.25 ± 0.04	0.25 ± 0.05	0.20 ± 0.05
	Female	6	0.23 ± 0.03	0.22 ± 0.02	0.22 ± 0.03	0.25 ± 0.03
		12	0.22 ± 0.06	0.22 ± 0.07	0.22 ± 0.07	0.21 ± 0.04
		22	0.20 ± 0.03	0.20 ± 0.03	0.20 ± 0.03	0.20 ± 0.03
Maximum indentation height, h_f (μm)	Male	6	27.28 ± 3.91	27.50 ± 3.73	26.33 ± 4.84	28.00 ± 3.58
		12	28.83 ± 7.32	27.83 ± 5.67	30.00 ± 9.01	28.67 ± 8.12
		22	26.52 ± 3.31	25.00 ± 2.24	27.29 ± 3.86	27.29 ± 3.55
	Female	6	26.56 ± 4.02	25.83 ± 3.43	27.67 ± 5.13	26.17 ± 3.82
		12	26.78 ± 3.96	28.00 ± 5.25	27.17 ± 4.17	25.17 ± 1.83
		22	25.13 ± 2.88	24.40 ± 2.07	24.80 ± 2.17	26.20 ± 4.21

also shows comparisons according to gender and the RPI method of calculating the area function applied.

Figure 7 shows the elastic moduli for the femurs of (*a*) HETcKO mice and (*b*) their littermate controls. Statistical analysis using one-way ANOVA and Tukey HSD test for post hoc comparisons indicated that there were no significant differences in the elastic moduli obtained from three-point bending versus the RPI technique (geometric method and O/P method).

Table 7 Elastic modulus values derived from the three experiments for both male and female mice in comparison with the control group values. The average and standard deviation values are noted.

4–5 month group modulus values	Control male	HETcKO male
Three-point bending (GPa)	5.28 ± 0.34	7.33 ± 1.13
RPI—geometric method (GPa)	5.61 ± 1.25	7.45 ± 0.86
RPI—O/P method (GPa)	5.53 ± 1.27	7.46 ± 0.92
	Control female	HETcKO female
3-pt bending (GPa)	5.26 ± 0.48	8.48 ± 0.48
RPI—geometric method (GPa)	5.04 ± 0.96	7.24 ± 1.11
RPI—O/P method (GPa)	4.93 ± 0.97	7.31 ± 1.09

4 Discussion

This study presents a numerical methodology to calculate the elastic modulus of mouse bones using a RPI technique. This technique includes two different methods for determining the area function, which are termed the O/P method and geometric method throughout this paper. Furthermore, a comparative study between the proposed RPI-based methodology and the traditional three-point bending methodology has been described.

We selected PMMA as a material to test initially as it had a modulus value in the range of values reported for mouse bones. While the values obtained from the proposed method compared well with what is known for the material, it must be noted that we could not perform a corresponding three-point bending test to obtain a comparative elastic modulus because the company could not provide samples used specifically for testing and because the PMMA modulus values would vary depending on the manufacturing process. However, we have noted that the elastic modulus values obtained using the proposed RPI technique are similar to what is reported in literature and it has been consistent throughout the various tests conducted on PMMA.

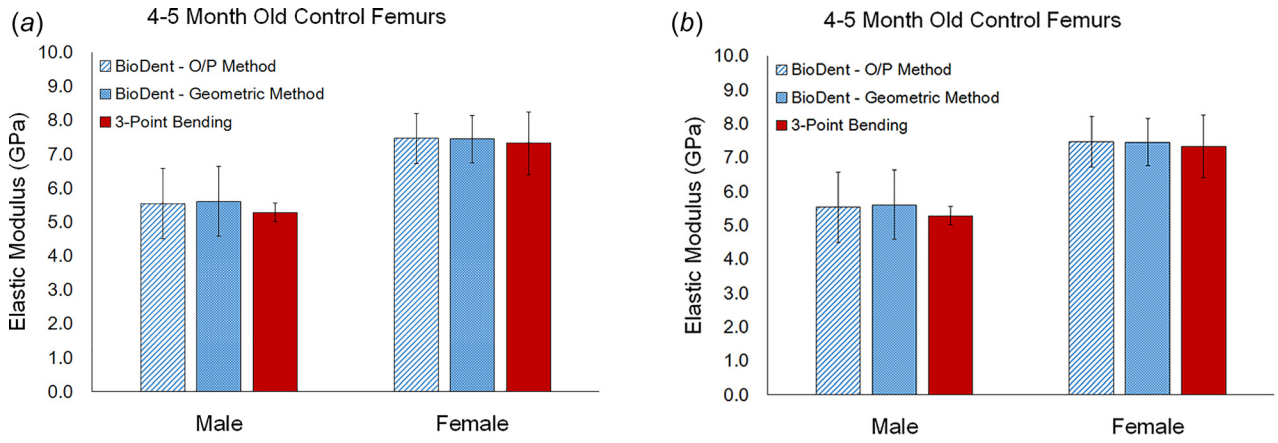

Fig. 7 Analysis of elastic moduli of femurs from (*a*) HETcKO mice and (*b*) their littermate controls revealed no significant differences in the elastic moduli, regardless of the analysis technique applied

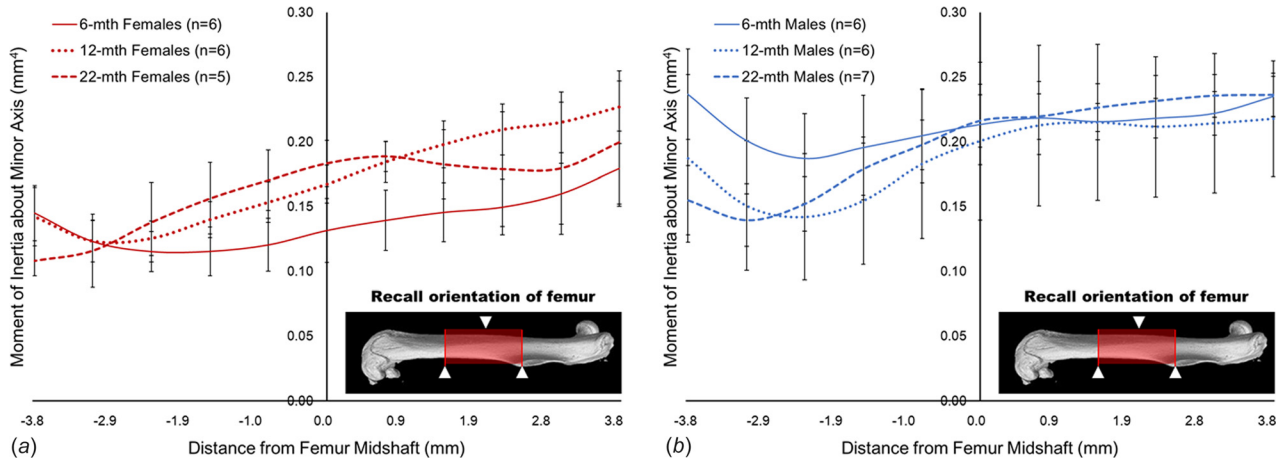

Fig. 8 Comparison of moments of inertia for C57BL/6 femurs by age in (*a*) females and (*b*) males. Distance measurements correspond to the total length of the 7.6 mm span. Negative values correspond to the distal direction while positive value correspond to the proximal direction with respect to the midshaft.

In order to test its applicability to murine bones, we then conducted the tests on the group 1 TOPGAL mice and while no three-point bending tests were performed on these samples, we looked at the SEM images from these bones at several indentation sites. As shown in Fig. 5, it is apparent that the indentation is clearly not fully elastic and that microdamage is evident at the indentation site. However, the assumption of an elastic rebound is made in this study when using the unloading slope for the calculation of the elastic indentation modulus. If this method is used for in vivo studies, it would be interesting to observe the bone remodeling process after an indentation at the microdamage site.

For the group 2 gender and aging study mice, the three-point bending moduli were consistently lower than the RPI moduli. One reason could be that the RPI modulus represents the elastic modulus of the material only at the site of the indentation, whereas the three-point bending modulus takes into account the architecture of the bone between the two supports; therefore, a lower elastic modulus would indicate that the bone has a higher average moment inertia value. After comparing the RPI moduli calculated using both the O/P and geometric methods, we found that the geometric method consistently computed RPI moduli that more closely matched the three-point bending moduli. The three-point bending procedure also accounted for the inherent architectural effects of the bones tested, whereas the RPI-based methodology did not. This observation was evident in the 22-month-old femurs, which exhibited a lower elastic modulus after we applied three-point bending but not after we applied the RPI technique. However, the RPI moduli still indicate that the bone material in the cortical region is similar in nature across aging.

From the observations on the unloading slope and maximum indentation height, it can be deduced that the RPI modulus was more greatly influenced by variations in the unloading slope than variations in the maximum indentation height. Future applications of this RPI-based methodology include the analysis of bone properties in mice through in vivo longitudinal studies and the collection of spatially specific elastic moduli to incorporate more heterogeneity in finite element models of the bone (i.e., assigning a distribution of the elastic modulus values throughout the finite element model).

Another important aspect that highlights the differences between the three-point bending procedure and the RPI technique is the role of the bone architecture in the computation of the three-point bending modulus. For all the samples in study 3, we studied the variation in the moment of inertia about the bending axis along the span of the specimen. Figure 8 shows the variation of the average of the sample values of the moment of inertia for each age and gender. The main observations based on gender were that males exhibited ~60% higher moment of inertia than females at 6 months. However, gender differences in moment of inertia were smaller at 12 and 22 months. For age-based differences, the

observation are that in females, moment of inertia at the midshaft increases with age while in males, moment of inertia at the midshaft is similar for the 6-month (0.214) and 22-month groups (0.216).

As the moment of inertia increases, the predicted elastic modulus decreases. Hence, it is likely that the higher elastic modulus predicted by the three-point bending tests for females at 6 months of age, as seen in Fig. 7, could be the result of the lower MOI for females seen at the same age as seen in Fig. 8. Because the differences in the moment of inertia values for other age groups and gender groups were minimal at either 12 or 22 months of age, we did not observe major differences in the elastic modulus values using either the three-point bending tests or the RPI technique (geometric method and O/P method). In particular, the RPI modulus is derived from a localized region (10–30 μm) and is likely representative of the local collagen/mineral structure and organization, thus discounting the effect of the overall architecture.

For the murine femurs tested in group 3, the deletion of a single allele of β-catenin in osteocytes (HETcKO) resulted in the rapid loss of trabecular bone in females and much slower trabecular loss in males [24,34]. However, the elastic modulus was tested in the mid-diaphysis region of the bone, which is predominantly cortical in nature. The elastic modulus compared well across three of the bones except in female HETcKO mice where the three-point bending showed a 17% higher value. The indentation modulus values for these mice were similar to those of the TOPGAL mice.

5 Conclusions

This paper presents a methodology for computing the elastic modulus using RPI, which employs micro-indentation principles, and includes two methods of computing the corresponding area function—namely the Oliver–Pharr method and the Geometric method has been outlined. This method has shown promise in various studies conducted on both PMMA and different types of mouse bones. The method is relatively easy to use and is nondestructive, thereby making it suitable to analyze one aspect of bone quality in longitudinal studies. Furthermore, in vivo studies can be performed on bones that are close to the skin such as the tibia. This study shows that applying the proposed RPI technique on mouse bones produces RPI moduli that are similar to the elastic moduli obtained from three-point bending. This RPI methodology is also able to capture differences in the material property at different indentation sites, thereby having the ability to characterize the heterogeneity of bone material. Although three-point bending tests computed the elastic modulus based on the architectural differences in the bone between the supports and captured the differences in the modulus across aging, the proposed method was not able to do so and computed an elastic modulus that represents the material property alone. While this paper presents the methodology and the results from testing across different murine bones, further research and experiments are required to verify and validate this method more rigorously.

Acknowledgment

The authors would like to thank the assistance of Dr. Vladimir Dusevich in helping us take the SEM pictures.

Funding Data

- Directorate for Engineering (NSF-CMMI/BMMB—No. 16622884 (Ganesh Thiagarajan—PI)).
- Foundation for the National Institutes of Health (NIA P01 AG039355 (LF Bonewald—PI)).
- National Institute of Arthritis and Musculoskeletal and Skin Diseases (NIAMS R01 AR053949 (ML Johnson—PI)).

References

[1] Jämsä, T., Jalovaara, P., Peng, Z., Väänänen, H. K., and Tuukkanen, J., 1998, "Comparison of Three-Point Bending Test and Peripheral Quantitative Computed Tomography Analysis in the Evaluation of the Strength of Mouse Femur and Tibia," Bone, **23**(2), pp. 155–161.

[2] Akhter, M., Raab, D., Turner, C., Kimmel, D., and Recker, R., 1992, "Characterization of In Vivo Strain in the Rat Tibia During External Application of a Four-Point Bending Load," J. Biomech., **25**(10), pp. 1241–1246.

[3] Akhter, M. P., Cullen, D. M., Gong, G., and Recker, R. R., 2001, "Bone Biomechanical Properties in Prostaglandin EP1 and EP2 Knockout Mice," Bone, **29**(2), pp. 121–125.

[4] Turner, C. H., 2006, "Bone Strength: Current Concepts," Ann. New York Acad. Sci., **1068**(1), pp. 429–446.

[5] van Lenthe, G. H., Voide, R., Boyd, S. K., and Müller, R., 2008, "Tissue Modulus Calculated From Beam Theory is Biased by Bone Size and Geometry: Implications for the Use of Three-Point Bending Tests to Determine Bone Tissue Modulus," Bone, **43**(4), pp. 717–723.

[6] Hansma, P. K., Turner, P. J., and Fantner, G. E., 2006, "Bone Diagnostic Instrument," Rev. Sci. Instrum., **77**(7), p. 075105.

[7] Beutel, B. G., and Kennedy, O. D., 2015, "Characterization of Damage Mechanisms Associated With Reference Point Indentation in Human Bone," Bone, **75**, pp. 1–7.

[8] Karim, L., Van Vliet, M., and Bouxsein, M. L., 2018, "Comparison of Cyclic and Impact-Based Reference Point Indentation Measurements in Human Cadaveric Tibia," Bone, **106**, pp. 90–95.

[9] Katsamenis, O. L., Jenkins, T., and Thurner, P. J., 2015, "Toughness and Damage Susceptibility in Human Cortical Bone is Proportional to Mechanical Inhomogeneity at the Osteonal-Level," Bone, **76**, pp. 158–168.

[10] Granke, M., Coulmier, A., Uppuganti, S., Gaddy, J. A., Does, M. D., and Nyman, J. S., 2014, "Insights Into Reference Point Indentation Involving Human Cortical Bone: Sensitivity to Tissue Anisotropy and Mechanical Behavior," J. Mech. Behav. Biomed. Mater., **37**, pp. 174–185.

[11] Granke, M., Makowski, A. J., Uppuganti, S., Does, M. D., and Nyman, J. S., 2015, "Identifying Novel Clinical Surrogates to Assess Human Bone Fracture Toughness," J. Bone Miner. Res., **30**(7), pp. 1290–1300.

[12] Diez-Perez, A., Güerri, R., Nogues, X., Cáceres, E., Peña, M. J., Mellibovsky, L., Randall, C., Bridges, D., Weaver, J. C., and Proctor, A., 2010, "Microindentation for In Vivo Measurement of Bone Tissue Mechanical Properties in Humans," J. Bone Miner. Res., **25**(8), pp. 1877–1885.

[13] Krege, J. B., Aref, M. W., McNerny, E., Wallace, J. M., Organ, J. M., and Allen, M. R., 2016, "Reference Point Indentation is Insufficient for Detecting Alterations in Traditional Mechanical Properties of Bone Under Common Experimental Conditions," Bone, **87**, pp. 97–101.

[14] Gallant, M. A., Brown, D. M., Organ, J. M., Allen, M. R., and Burr, D. B., 2013, "Reference-Point Indentation Correlates With Bone Toughness Assessed Using Whole-Bone Traditional Mechanical Testing," Bone, **53**(1), pp. 301–305.

[15] Allen, M. R., Newman, C. L., Smith, E., Brown, D. M., and Organ, J. M., 2014, "Variability of In Vivo Reference Point Indentation in Skeletally Mature Inbred Rats," J. Biomech., **47**(10), pp. 2504–2507.

[16] Carriero, A., Bruse, J. L., Oldknow, K. J., Millán, J. L., Farquharson, C., and Shefelbine, S. J., 2014, "Reference Point Indentation is Not Indicative of Whole Mouse Bone Measures of Stress Intensity Fracture Toughness," Bone, **69**, pp. 174–179.

[17] Allen, M. R., McNerny, E., Organ, J. M., and Wallace, J. M., 2015, "True Gold or Pyrite: A Review of Reference Point Indentation for Assessing Bone Mechanical Properties In Vivo," J. Bone Miner. Res., **30**(9), pp. 1539–1550.

[18] Idkaidek, A., Agarwal, V., and Jasiuk, I., 2017, "Finite Element Simulation of Reference Point Indentation on Bone," J. Mech. Behav. Biomed. Mater., **65**, pp. 574–583.

[19] Jenkins, T., Coutts, L., Dunlop, D., Oreffo, R., Cooper, C., Harvey, N., and Thurner, P. J., 2015, "Variability in Reference Point Microindentation and Recommendations for Testing Cortical Bone: Maximum Load, Sample Orientation, Mode of Use, Sample Preparation and Measurement Spacing," J. Mech. Behav. Biomed. Mater., **42**, pp. 311–324.

[20] Jenkins, T., Katsamenis, O., Andriotis, O., Coutts, L., Carter, B., Dunlop, D., Oreffo, R., Cooper, C., Harvey, N., and Thurner, P., 2017, "The Inferomedial Femoral Neck is Compromised by Age But Not Disease: Fracture Toughness and the Multifactorial Mechanisms Comprising Reference Point Microindentation," J. Mech. Behav. Biomed. Mater., **75**, pp. 399–412.

[21] Oliver, W. C., and Pharr, G. M., 1992, "An Improved Technique for Determining Hardness and Elastic Modulus Using Load and Displacement Sensing Indentation Experiments," J. Mater. Res., **7**(6), pp. 1564–1583.

[22] Randall, C., Mathews, P., Yurtsev, E., Sahar, N., Kohn, D., and Hansma, P., 2009, "The Bone Diagnostic Instrument III: Testing Mouse Femora," Rev. Sci. Instrum., **80**(6), p. 065108.

[23] Lara-Castillo, N., Kim-Weroha, N., Kamel, M., Javaheri, B., Ellies, D., Krumlauf, R., Thiagarajan, G., and Johnson, M., 2015, "In Vivo Mechanical Loading Rapidly Activates β-Catenin Signaling in Osteocytes Through a Prostaglandin Mediated Mechanism," Bone, **76**, pp. 58–66.

[24] Javaheri, B., Stern, A. R., Lara, N., Dallas, M., Zhao, H., Liu, Y., Bonewald, L. F., and Johnson, M. L., 2014, "Deletion of a Single Beta-Catenin Allele in Osteocytes Abolishes the Bone Anabolic Response to Loading," J. Bone Miner. Res., **29**(3), pp. 705–715.

[25] Lu, Y., Thiagarajan, G., Nicolella, D. P., and Johnson, M. L., 2012, "Load/Strain Distribution Between Ulna and Radius in the Mouse Forearm Compression Loading Model," Med. Eng. Phys., **34**(3), pp. 350–356.
[26] Begonia, M. T., Dallas, M., Vizcarra, B., Liu, Y., Johnson, M. L., and Thiagarajan, G., 2015, "Non-Contact Strain Measurement in the Mouse Forearm Loading Model Using Digital Image Correlation (DIC)," Bone, **81**, pp. 593–601.
[27] Carriero, A., Abela, L., Pitsillides, A. A., and Shefelbine, S. J., 2014, "Ex Vivo Determination of Bone Tissue Strains for an In Vivo Mouse Tibial Loading Model," J. Biomech., **47**(10), pp. 2490–2497.
[28] Oliver, W. C., and Pharr, G. M., 2004, "Measurement of Hardness and Elastic Modulus by Instrumented Indentation: Advances in Understanding and Refinements to Methodology," J. Mater. Res., **19**(1), pp. 3–20.
[29] Carter, D. R., MikiC, B., and Padian, K., 1998, "Epigenetic Mechanical Factors in the Evolution of Long Bone Epiphyses," Zool. J. Linn. Soc., **123**(2), pp. 163–178.
[30] Shahar, R., Zaslansky, P., Barak, M., Friesem, A. A., Currey, J. D., and Weiner, S., 2007, "Anisotropic Poisson's Ratio and Compression Modulus of Cortical Bone Determined by Speckle Interferometry," J. Biomech., **40**(2), pp. 252–264.
[31] Doube, M., Kłosowski, M. M., Arganda-Carreras, I., Cordelières, F. P., Dougherty, R. P., Jackson, J. S., Schmid, B., Hutchinson, J. R., and Shefelbine, S. J., 2010, "BoneJ: Free and Extensible Bone Image Analysis in ImageJ," Bone, **47**(6), pp. 1076–1079.
[32] Abràmoff, M. D., Magalhães, P. J., and Ram, S. J., 2004, "Image Processing With ImageJ," Biophotonics Int., **11**(7), pp. 36–42.
[33] Ferguson, V. L., Ayers, R. A., Bateman, T. A., and Simske, S. J., 2003, "Bone Development and Age-Related Bone Loss in Male C57BL/6J Mice," Bone, **33**(3), pp. 387–398.
[34] Kramer, I., Halleux, C., Keller, H., Pegurri, M., Gooi, J. H., Weber, P. B., Feng, J. Q., Bonewald, L. F., and Kneissel, M., 2010, "Osteocyte Wnt/β-Catenin Signaling is Required for Normal Bone Homeostasis," Mol. Cell. Biol., **30**(12), pp. 3071–3085.